



MACHINA, the Movable Accelerator for Cultural Heritage In-situ Non-destructive Analysis: project overview

F. Taccetti¹ · L. Castelli¹ · M. Chiari¹ · C. Czelusniak¹ · S. Falciano^{2,3} · M. Fedi¹ · F. Giambi^{1,4} · P. A. Mandò^{1,4} · M. Manetti¹ · M. Massi¹ · A. Mazzinghi^{1,4} · C. Ruberto^{1,4} · P. Ronzino⁵ · I. Bini¹ · S. Frati¹ · F. Benetti⁶ · M. Cestelli Guidi⁶ · M. Ciatti⁷ · C. Frosinini⁸ · S. Rossi⁸ · S. Mathot⁹ · G. Anelli⁹ · G. Cipolla⁹ · A. Grudiev⁹ · A. Lombardi⁹ · E. Milne⁹ · E. Montesinos⁹ · H. Pommerenke⁹ · K. Scibor⁹ · M. Vretenar⁹ · L. Giuntini^{1,4}

Received: 21 October 2022 / Accepted: 24 November 2022 / Published online: 15 March 2023
© The Author(s) 2023

Abstract

Over the years, transportable instrumentation for cultural heritage (CH) in situ measurements has noticeably widespread, due to logistic, economical and safety reasons. Ion beam analysis, a powerful set of analytical techniques, of great importance for CH, is instead carried out by using fixed instrumentation. To overcome this limit, the Italian national Institute of Nuclear Physics (INFN), CERN (European Centre for Nuclear Research) and the Opificio delle Pietre Dure (OPD), started MACHINA, the “Movable Accelerator for CH In-situ Non-destructive Analysis: the new generation of accelerators for art” to build a transportable accelerator, compact, with strongly reduced weight, absorbed power and cost. MACHINA will be installed at the OPD and dedicated to CH. It will be moved to major conservation centres and museums, when needed. The INFN-CERN proposal, approved in December 2017, became operative in February 2018. 2018 was dedicated to the acquisition of material/instrumentations, to set up both a dummy accelerator (to test the vacuum system) and a vacuum chamber (to test the source). Due to COVID, in 2020 and 2021 the experimental work was slowed down, but we kept developing the control electronics/software and built the second-generation supporting structure. The HF-RFQ power supplies were integrated in October 2021. At the rise of 2022, after conditioning the cavities, we tested the system and in March 2022 we got the first extracted 2-MeV proton beam. In this paper, we present the structure of the MACHINA system, the approach followed and the main solutions adopted, with a special focus on the control system, and finally the first experimental results.

Keywords Transportable accelerator · Ion beam analysis · IBA · RFQ · Transportable instrumentation · Cultural heritage

✉ C. Czelusniak
czelusniak@fi.infn.it

✉ L. Giuntini
giuntini@fi.infn.it

¹ Istituto Nazionale di Fisica Nucleare, Sezione di Firenze, 50019 Sesto Fiorentino, Italy

² Istituto Nazionale di Fisica Nucleare, Sezione di Roma, 00185 Rome, Italy

³ Gran Sasso Science Institute, L'Aquila, 67100 L'Aquila, Italy

⁴ Dipartimento di Fisica e Astronomia, University of Florence, 50019 Sesto Fiorentino, Italy

⁵ PIN S.c.r.l.-Polo Universitario Città di Prato, Servizi Didattici e Scientifici Per l'Università di Firenze, I-59100 Prato, Italy

⁶ Istituto Nazionale di Fisica Nucleare, Laboratori Nazionali di Frascati, 00044 Frascati, RM, Italy

⁷ Accademia Nazionale dei Lincei, 00165 Rome, Italy

⁸ Opificio Delle Pietre Dure, Via Alfani, 78-50121 Florence, Italy

⁹ CERN–European Organization for Nuclear Research, CH-1211 Geneva 23, Switzerland

1 Introduction

In recent years, the growing interest in the analytical study of art-historical and archaeological artefacts has driven R & D to results of impact on Heritage Science. In particular, we have seen a noticeable development of transportable instrumentation for in situ measurements (Alfeld and Viguerie 2017; Pouyet et al. 2020; Ravaud et al. 2018; Taccetti et al. 2019; Oliveira et al. 2022; D’Alvia et al. 2022; Romano et al. 2012; Riminesi et al. 2022).

This kind of instrumentation is of great importance for cultural heritage (CH) diagnostics, because moving precious and fragile objects, even over short distances, is always difficult and often becomes impossible, due to obvious logistic, economical and safety reasons.

Traditionally, ion beam analysis (IBA) is carried out using fixed instrumentation installed in nuclear physics laboratories. To overcome this limit, the Italian national Institute for Nuclear Physics (INFN), together with CERN (European Centre for Nuclear Research) in Geneva and the Opificio delle Pietre Dure (OPD) in Florence, developed MACHINA (Movable Accelerator for CH In-situ Non-destructive Applications), a complete transportable IBA system, which can be directly used in conservation centres and museums for CH applications. This project allows combining in the same system the IBA strong points (e.g. high sensitivity, non-invasiveness, non-destructiveness, simultaneous use of complementary techniques, etc.) and transportability, a feature strongly contributing to the great diffusion of techniques such as, for example, XRF or Raman spectroscopy in the CH field (Liss and Stout 2017; Defeyt et al. 2017; Mazzinghi et al. 2021; Gilbert et al. 2003; Marucci et al. 2018; Jehlička and Culka 2022; Rousaki and Vandenabeele 2021; Vandenabeele and Donais 2016; Senesi et al. 2021; Awad and Baias 2020).

MACHINA is a realistic compromise between a “perfect tool” for IBA compositional diagnostics in the CH field (Dran et al. 2004; Calligaro et al. 2020; Chiari et al. 2021) and a movable instrument, featuring just what is needed to answer the questions put by restorers.

MACHINA has been designed to be an open system and a transportable instrument. The present version allows for in situ X-rays (PIXE, Particle Induced X-rays Emission) and low-energy gamma-rays (PIGE, Particle Induced Gamma-rays Emission) detection. In the next future, the system is going to integrate different detectors for making additional IBA techniques available, such as, for example, Ionoluminescence (IL). MACHINA produces 2-MeV pulsed proton beams with maximum mean intensity of a few nA, typically an order of magnitude higher than the typical currents adopted for IBA studies of CH.

MACHINA is a *green* instrument, with a very low impact under all the aspects (absorbed power, footprint, weight, components availability, cost, radiation emission, noise) with respect to conventional IBA systems, thus making the system accessible to a much wider community than the present one, in particular to stakeholders with limited budget.

MACHINA will be housed at the OPD, a world-renowned centre for art conservation. The application of the IBA techniques where artworks are studied and conserved allows for measurements on a variety of objects that would be otherwise impossible to analyse. However, when needed, it will be also possible to move MACHINA for in situ measurements, e.g. at museums or conservation sites.

Here, after an introduction about the motivations of MACHINA, the structure of the MACHINA system, the approach followed and the main solutions adopted, with special focus on the control system, together with the first experimental results are presented.

2 Motivations of the MACHINA project

Scientific diagnostics for CH have gained a lot in the recent past, in terms of quantity, quality and acknowledged importance. Among the employed techniques, those based on the use of MeV particle accelerators have been playing a crucial role, as they allow reconstructing surface composition and structure of the used materials. This is accomplished by exploiting the spectroscopy of the particle-induced radiation emitted by the atoms (e.g. X-rays and visible light) or nuclei (gamma rays or particles) involved in interactions with the impinging beam particles, most often protons or alpha particles.

The IBA techniques allow for quantitative analyses, with minimum detection limits that can be in the ppm range. IBA analyses can be carried out in a non-invasive and non-deliberately destructive way, with the sample in the atmosphere. With the IBA techniques, the probed depth is well defined and typically ranges from a few tens of micrometres up to a few hundreds of micrometres, depending on the sample, the ion species and the beam energy. As a result, the probed depth can be easily tailored to the specific problem by choosing the proper ion and energy combination. All these features make IBA analyses of great importance for the study of CH over a wide time-span, from ancient times to present (see, for example, in the case of paintings and drawings (Olsson et al. 2018; A.-M.B Olsson et al. 2001; Roascio et al. 2002; Duval et al. 2004; Milota et al. 2008; Grassi et al. 2005; Grassi 2009; Zucchiatti et al. 2015) just to name a few).

However, although of great importance for the conservators, and art historians, only rather rarely IBA can be

performed on masterpieces. As mentioned above, at present, accelerators for IBA applications are designed to be installed in nuclear physics laboratories and cannot be either part of the scientific instrumentation of conservation centres and museums nor be transported where artworks are conserved. Nowadays, the masterpiece to be analysed with IBA techniques has to be in a conservation state good enough to allow moving it without significant risk of damaging; its dimensions are to be small, to make both the transport and the handling for the IBA analysis easy; the owners have to allow moving the artworks from the restoration centre to the IBA laboratory; it must be possible to pay transport and insurance costs, where the latter can be exceedingly high for many of the most famous masterpieces.

The MACHINA project is born to make the IBA techniques available for in situ analyses with a transportable system, thus joining IBA analysis and portability. To carry out the project, it has been necessary to tackle many critical issues, such as low weight, small form factor, low power consumption, low radioprotection impact, low cost, transportability, and ease of use. In the following, the adopted solutions and the obtained results are shortly presented.

3 Scheme of the MACHINA system

MACHINA's main blocks are:

Accelerator

1. Source and low-energy beam transfer (LEBT) line
2. Accelerator (HF-RFQ)
3. High-energy beam transfer (HEBT) line

Accelerator ancillaries

1. Vacuum
2. RF power supplies

Radio Safety

Control System

The source and the beam transfer lines at both low- and high-energy sides (LEBT and HEBT) have been designed to be as simple and compact as possible. As a whole, source, LEBT and HEBT are about 1.5 m long and absorb less than 1 kW at regime conditions. The two High Frequency-Radio Frequency Quadrupole (HF-RFQ) cavities, designed and machined at CERN⁴, are 0.5 m long each and have a 100-kg mass. As a whole, the accelerator system has a mass of less than 500 kg, a footprint of about 2.5 m × 1 m (length, along the beam axis, × width), and a mean power consumption of less than 1 kW.

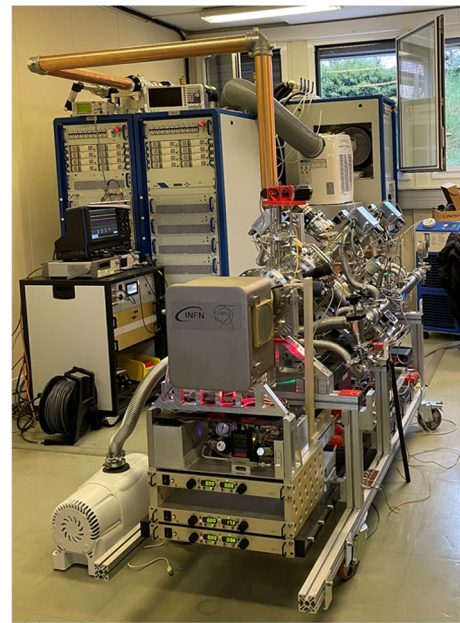


Fig. 1 A view of the MACHINA system during the tests at CERN. From left: the half rack holding the signal and waveform generators and hosting the module in charge of limiting the power injected into the cavities in case of exceedingly high pressure (higher than 10^{-5} mbar) in the accelerator; the two racks (blue frames) of the amplifiers of the RF PS from which the copper waveguide connects the RF PSs to the cavities; the accelerator assembly (foreground the metal cage of the source and the HV power supplies switched on). In the background: the chillers for the cavities and for the RF PSs

The RF-PS ensemble is composed of two 19"-width, 600 mm-depth racks for each RF unit, one half-rack for the control system, and one cooling unit, plus water ducts and electrical connections. In the present version, the RF power supply system has a mass slightly less than 900 kg, a footprint of 3.5 m × 1 m, and an absorbed power of about 14 kW.

Summarising, the MACHINA system is composed of independent elements that can be moved separately, has an overall footprint of less than 10 m², a mass less than 1400 kg, and absorbs about 15 kW.

In Fig. 1 and Fig. 2, the MACHINA system is shown. From now on, the names of the elements displayed in the control panel (see Sect. 5) are reported in *italics*.

3.1 SOURCE and LEBT

MACHINA makes use of a proton radio frequency (RF) source, based on a standard NEC RF source. RF sources are better suited to the MACHINA project with respect to other sources, e.g. Duoplasmatron or Sputter sources (two sources widely used in IBA accelerators), due to lower weight and smaller dimensions, lower absorbed power, no need of liquid cooling, absence of dangerous/poisoning substances (such

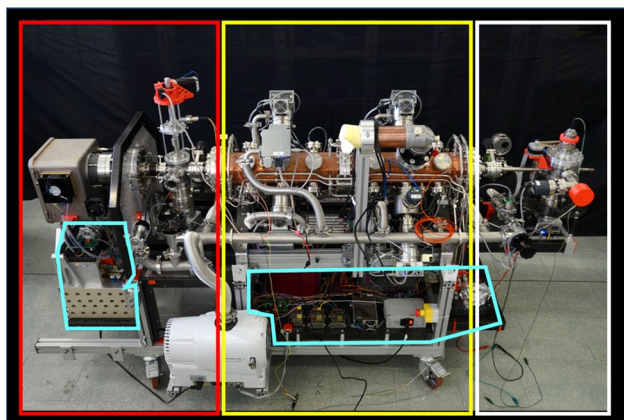


Fig. 2 Side view of MACHINA showing all the sections. Red frame: source and LEBT, yellow: HF-RFQ, white: HEBT, cyan: control electronics

as Li, Rb or Cs), lower high voltages, and longer intervals between maintenance interventions.

The gas circuit has been fully redesigned and optimised for our application. Hydrogen gas is stored in a solid metal-hydride cartridge (10 cm × 3 cm) at high pressure (30 bar). Stainless-steel pipes were used for reducing leaks.

Downstream of the gas cartridge, we have a manual pressure reducer, which lowers hydrogen pressure to less than 2 bars; then, gas is fed to an Alicat Mass Flow controller, set typically at some percent (5–10%) of the full scale (2 sccm).

Successively, a Pirani gauge allows monitoring the gas pressure, typically around 1 mbar, when the source is running (*Gas Inlet* $x, y E + w z$ mbar).

The gas load from the source is expected to be in the low part of 10^{-3} mbar/l/s. Simulations have shown that the operating vacuum inside the HF-RFQ (10^{-5} mbar scale or better) can be obtained with the 9 turbo pumps installed on MACHINA. The experimental results confirmed the simulations (see Sect. 3.4.1).

Four electromagnetic valves (no compressed air needed to activate them) *V1*, *V2*, *V3* and *V4* allow either the gas to flow into the source quartz bottle or to connect the gas line to an external HV system (to remove air from the gas pipes after installing the high-pressure gas vessel). In this operation, a manual valve just after the high-pressure vessel avoids emptying it.

When the gas is flowing, switching on the 100 MHz, 525 V, RF power supply (PS) (*RF_PS power*), capacitively coupled to the source vessel (quartz bottle), allows plasma formation (as shown in Fig. 3) and thus creating the beam. Source cooling is provided by a fan (RF Fan 2600 rpm).

Three high voltages are used to operate the source. The probe voltage (*HV_Probe*) is used to help ion drift towards the bottle exit canal. The extraction voltage *HV_Extraction* allows pulling the particles out of the source. The sum of

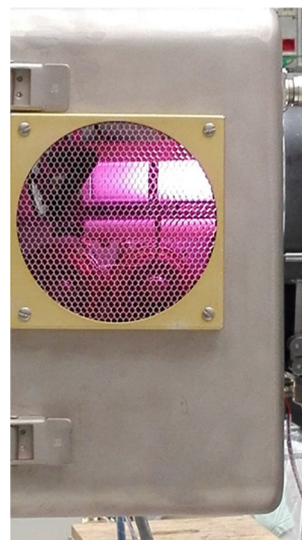


Fig. 3 The RF source switched on. It is possible to see the quartz bottle, where the bright light comes from, and one of the bands for the capacitively coupling, on the left-hand side of the brighter region of the ionised gas. The cooling fan is installed on the other side and is not visible here

HV_Probe and *HV_Extraction* determines the accelerating voltage and thus the energy of the beam particles, set at 20 keV (100 eV spread), as required by the RFQ cavity specifications for acceleration.

Just downstream of the exit of the source extraction canal, the Einzel lens assembly is installed, to allow focusing the beam at the entrance of the accelerator. The third high-voltage *HV_Einzel* is applied to the central electrode of the Einzel lens.

The elements of the source are either on the deck at ground potential (*GND-DECK*) or at the extraction voltage (*HV-DECK*). The former are the extraction and the Einzel lens PS; the latter, all the elements of the gas circuit and of the source itself (e.g. RF PS, fan, control boards, probe PS). These elements are powered via an insulated transformer.

The characteristics of the source are in very good match with those of the accelerator. Actually, the calculated RFQ acceptance is $\epsilon_{\text{tot}} = 30 \pi$ mm mrad (total), while the given emittance of the source at 20 keV is $\epsilon_{\text{tot}} = 28 \pi$ mm mrad (total). Simulations, later confirmed by experimental tests, have shown that direct beam injection into the RFQ accelerator is possible and no active elements are required.

As a consequence, the LEBT assembly has been designed to be as simple and compact as possible. An edge-welded bellow is the first element of this section, and it allows adjusting the source and LEBT mutual positions and alignment. After, we find a 6-way cross, holding:

- The vacuum turbo pump VS1,

- A quartz window, for checking the correct positioning of the Faraday Cup (FC),
- A compact full-range gauge (Agilent FRG-700, *HVI*), to measure the residual gas pressure (from atmosphere down to 5×10^{-9} mbar) in this section, essentially determined by the gas leak from the source,
- The remotely controlled Faraday Cup (*FC* in the control panel), to measure the beam intensity just downstream of the source, prior to the injection into the accelerator. The FC is normally inserted on the beam path and can be extracted only by activating the FC stepper motor. Indeed, a ~ 20 -N force (created by the external air pressure) causes the FC to be quickly inserted along the beam path. In this way, the beam can be accelerated if and only if all the radioprotection interlock allows powering the motor and removing the FC from the beam path.

Downstream of this element, the first manual gate valve allows separating the LEBT and accelerator sections.

3.2 HF-RFQ accelerator

The design of the high-frequency-radio frequency quadrupole accelerator has been strongly inspired by the first HF-RFQ developed at CERN for medical applications (Lombardi et al. 2015; Dimov et al. 2018). For MACHINA, an optimised HF-RFQ (called PIXE-RFQ) has been designed by considering the lowest possible injection in a 750-MHz RFQ combined with a sufficient transverse acceptance to generate a pulsed 2-MeV proton beam with a sufficiently small emittance to be focused without excessive collimation (less than 20%) to a beam spot size of about 500 μm in diameter. The result is a 1-m-long HF-RFQ, able to accelerate to 2 MeV and focus the 20 keV proton beam produced by the source, using a vane voltage of only 35 kV. The repetition rate is 200 Hz, and the pulse length 125 μs , (2.5% duty cycle).

The construction process and all the details of the PIXE-RFQ are described in Mathot et al. (2019). We will remind here only the essentials.

As regards the vacuum connection ports, the cavities have two DN100CF flanges at the two ends for coupling the accelerator to the LEBT and HEBT sections, while DN40CF and DN16CF connections are used for services.

Concerning the twenty-four DN40CF ports:

- One is used for the single-input power coupler, for the RF power injection connection,
- Sixteen host the tuners of fixed length (eight per module, in axial-symmetric arrangement), used both to tune the cavity to the operating frequency and to flatten the field by adjusting their penetration into the cavity volume. The

goal is to suppress dipole components of the field and obtain a pure quadrupolar field,

- On the remaining seven ports, the *VS2-VS8* turbo pumps are installed. For two of them (*VS2* and *VS6*), a tee piece is installed between the port and the pump. Here two FRGs are installed, *HV2@VS2* (at the beginning of the first cavity) and *HV2@VS6* (at the end of the second module) to measure the pressure along the accelerator.

As regards the eight DN16CF ports:

- Four of these ports are used for diagnostic RF pickup antennas, to measure the amplitude of the magnetic field in the RFQ cavities, and thereby the inter-vane voltage, during operation,
- The other four ports are not used.

During operations, the cavities are cooled by two independent water circuits built inside the cavities themselves. The inner part of each cavity (the vane) is cooled by a 5-mm-diameter duct, while the outer part (the body) by an 8-mm-diameter pipe. The cooling channels of the two modules are connected in series and the four channels of each diameter per module in parallel. The two lines are connected to the first chiller, able to provide the required water flow for the two lines, typically around 13 and 5 l/s, respectively.

The RF power can be applied to the cavities and the beam can be accelerated only if the residual gas pressure, as measured by the FRG *HV2@VS6*, is sufficiently low to switch off the RF-PS safety interlock.

The cavities supporting structure has been built using carbon fibre bars that hold together sturdy, carved, aluminium trapezoidal frames. All these elements are mounted on a robust and lightweight structure made of 50 mm \times 50 mm aluminium profiles, under which four wheels allow for easy transport of the MACHINA accelerator. A carbon fibre sheet sits on the lower part of the aluminium structure and holds the low-voltage power supplies (+24 V, +12 V, +5 V, +3.3 V, -12 V) and their distribution rails, the transformer for powering the HV deck and most of the boards of the control system (Arduino microcontrollers and the boards to communicate with the instrumentation), the remaining boards being mounted on two smaller carbon fibre sheets just underneath the cavities.

3.3 HEBT

At the exit of the second accelerating module, a second manual gate valve is installed, to separate the accelerator from the HEBT section. After the valve, a drift pipe is placed, where a pair of permanent quadrupole magnets (PMQs) can be installed, to focus the beam down to a few hundreds of micrometres.

After the drift, the beam passes through the high-energy diagnostic station. It consists of a UHV, 100-mm-diameter, 100-mm height chamber. Here, a remotely controlled, rotatable carousel allows for the insertion of: (i) a Faraday Cup and Beam Stopper (*HE-FC*), (ii) a quartz, to visualise shape, intensity, and position of the beam, (iii) 1 thinner foil, to reduce beam energy from 2 MeV down to around 1.5 MeV, (iv) 1 thicker foil, to reduce beam energy to around 1 MeV, (v) two blank positions, at 180° with respect to each other, to let the beam proceed towards the target. Under the chamber, the last turbo pump, indicated as *VS9*, is installed.

On the lateral ports of the chamber, we find: (i) a manual valve, which opens/closes the low-speed pump-down line (see below), (ii) an FRG vacuum gauge (*HV3*), (iii) a viewport for a remotely controlled led system, which allows seeing inside the chamber, (iv) a viewport for TV camera.

On top of the diagnostic chamber, a remotely controlled stepper motor allows for rotating the internal carousel and thus setting the desired item onto the particle path.

For the extraction of the ions into the atmosphere and for counting the X-rays produced by the beam in the extraction window (see below), a snout, whose features are shown in Fig. 4, has been designed and constructed using metallic additive manufacturing (3D print) (Grazzi et al. 2021).

The accelerated particles move along the main axis of the snout and eventually pass through the extraction window, glued on the tip of the snout. In this way, they can be extracted into air and reach the sample, which is set at a distance between 6 and 10 mm from the window. For the extraction window, a silicon nitride (Si_3N_4) membrane, 0.5 μm thick, is used. The low Z and the noticeable thinness strongly limit beam degradation (energy loss, straggling and beam widening) and the production of radiation (mainly X and gamma rays) due to the interaction of the particles in the window. This latter point is of great importance, as it allows minimising background in PIXE/PIGE measurements. Si_3N_4

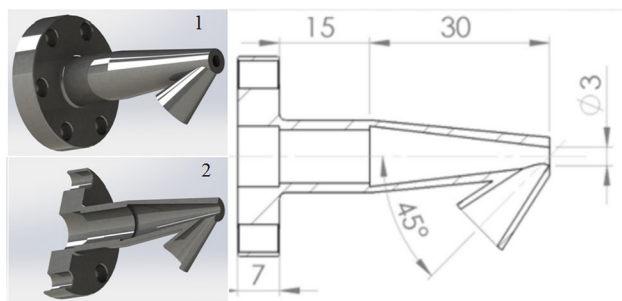


Fig. 4 The final part of the MACHINA beamline. Beam particles move along the straight structure and finally reach the tip of the structure, where the Si_3N_4 extraction window is installed. The inclined cone is exploited for detecting the X-rays produced by the beam in the exit window and subtends the SDD detector (not shown) for indirect current detection

windows are resistant enough to withstand the passage of the proton beams for years, practically without any damage, and allow maintaining a high-vacuum regime in the region before the window. At the INFN-LABEC, Si_3N_4 windows have been routinely used on all the external beam lines over the past twenty years without any problem (Lucarelli et al. 2018).

A 0.5- μm Si_3N_4 membrane induces small energy loss (~ 22 keV) and straggling (~ 3.5 -keV FWHM) with respect to the contribution of 6–10 mm in air of a 2-MeV proton beam (of the order of 100–170 keV energy loss and 7–9 keV energy straggling, respectively, SRIM simulation (Ziegler et al. 2010)). Its contribution as energy straggling is also negligible with respect to the one induced by the acceleration process (about 10 keV).

The Si_3N_4 window also allows for indirect counting of the number of particles hitting the target during a measurement. Indeed, as the beam energy (2 MeV) and the window thickness (0.5 μm) are fixed, the number of Si X-rays produced in the window is proportional to the number of particles hitting the window. A dedicated X-ray detector aiming at the beam impact point on the window allows for counting the so produced Si X-rays and thus the number of protons hitting the target (Giuntini et al. 2007).

The PIXE-PIGE detection set-up is not described in this paper, as it will be presented together with the acquisition program; the whole system (acquisition and detectors) is presently under test. However, it is based on two X-ray detectors and one gamma ray detector, a configuration typically adopted in our laboratory (Lucarelli et al. 2018; Giuntini et al. 2007). One more X-ray detector is used for indirect beam charge normalisation, as described above. The four detectors are extremely compact and have the same geometry. The X-ray detectors have the same specifications of those adopted for our XRF scanner (Taccetti et al. 2019).

3.4 Accelerator ancillaries

In this section, the two main sections of services for the MACHINA system are described: the vacuum and the cavity power supply assembly.

3.4.1 Vacuum

The vacuum system is based on nine turbopumps Agilent TwissTorr FS 84 (56 L/s actual pumping speed in air at regime conditions) and one Agilent IDP 10 scroll pump (10 m^3/h nominal pumping speed). The turbopumps are compact (97 mm diameter, 170 mm height), lightweight (less than 4 kg each, overall) and show good resistance to shocks, all features of crucial importance to make MACHINA a truly transportable system. The whole set of pumps has shown no

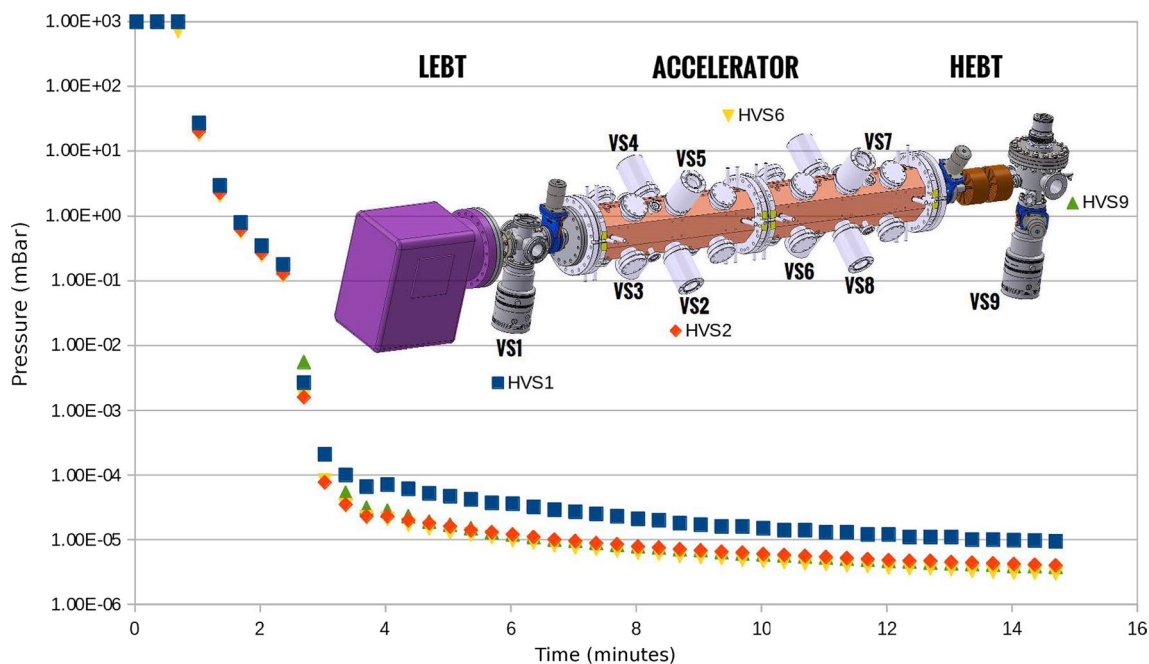


Fig. 5 Test of the vacuum system. Regime values have been assumed as the pressure values after about 15 minutes. HVS1 (blue), HVS2 (red), HVS6 (yellow), and HVS9 (green) are the pressure values in

the LEBT just after the source, at the beginning of the first cavity, at the end of the second cavity, and at the HEBT diagnostic chamber, respectively

problems after the many thousands of km travelled back and forth between LABEC and CERN.

All the nine VS have a common exhaust line, 40 mm diameter. This runs all around the accelerator and collects the nine DN16KF forelines of the VSs. This line is fed to the forepump, a 10 m³/h dry scroll pump, 25 kg mass, which, in a few minutes, allows reaching the 10⁻³ mbar pressure range in the whole beamline. An electromagnetic valve, installed on the inlet of the scroll pump, protects the system against sudden venting in case of power loss (the solenoid valve closes in 20 ms). We have four Pirani gauges to measure the pressure along this pipe, one in the LEBT, two in the accelerator, and one in the HEBT section, respectively.

The vacuum regime inside the RFQ was expected to be at least in the 10⁻⁶ mbar scale, as required for a safe working of the RFQs. Tests have shown that the minimum achievable pressure in the cavities is definitely lower than this limit, also when both the LEBT and HEBT sections are in communication with the accelerator (notwithstanding the gas load from the source in the LEBT and from the Si₃N₄ window in the HEBT).

The above results show that the regime pressure is well within the design value in all the sections of the beamline, with the pressure in the cavities (red and yellow lines) one order of magnitude lower than the design values.

As shown in Fig. 5, the accelerator is operative (residual pressure in the 10⁻⁶ mbar scale) in about 15 minutes after switching on the vacuum system from ambient pressure.

This is an important result, in view of the actual use of MACHINA for in situ analyses, when the available time for the measurements may be quite short.

As detailed in the previous paragraph, the exit snout of the HEBT section is equipped with a 500-nm-thick Si₃N₄ window, which is very fragile and easily breaks in a normal pump-down. To overcome this problem, the HEBT diagnostic chamber has a line allowing for an ultra-slow pump-down of this part of the accelerator. This line is equipped with a UHV valve, just after the chamber, a DN16KF bellow, a Bourdon needle-dial pressure gauge (a few mbar sensitivity), a variable leak valve and a rough pump. The leak valve allows for finely changing the gas flow from the HEBT to the preliminary pump, while the Bourdon gauge allows controlling how quickly the pressure is being reduced in the chamber. Typically, a pumping speed of a few mbar/s is used, which guarantees a safe operation and allows reaching about 1 mbar in about 10 min and the 10⁻² mbar range in around 15 min. At this pressure, the VS9 turbo pump can be safely switched on and enter the 10⁻⁶ mbar scale in a few minutes.

3.4.2 RF-power supplies

DB Elettronica—Science Solutions ended the production of the Solid State Power Amplifier (SSPA) RF amplifier in mid-2021 and just in the fall of 2021 the SSPA was installed on MACHINA.

The SSPA system consists of two 38-unit racks, each containing 8 amplifiers in addition to the control system, plus two 28-unit racks for the heat exchanger (chiller), the RF signal generation system (waveform generator and RF signal generator), the LQD pressure interlock system and the electrical distribution of the SSPA. The whole system has a mass of slightly less than 900 kg, a footprint of $3.5\text{ m} \times 1\text{ m}$ and a power consumption of about 14 kW. All elements are independent from each other and are mounted on wheels to ensure transportability.

The system is based on a waveform generator, an RF signal generator, and an RF power amplifier. The waveform generator defines the duty-cycle parameters (e.g. pulse of 125 μs every 5 ms); the output controls the 750-MHz RF signal generator, which supplies the low-level signal to the RF amplifier (SSPA). The amplifier, consisting of 8 RF modules contained in two racks, is capable of providing 100 kW pulse power. The SSPA unit feeds the RFQs through a single $3 + 1/8$ " copper coaxial RF line. The combination of the SSPA unit and the RFQ unit creates the paddle acceleration voltage (35 kV) within the cavities. The system is designed to provide a peak power of up to 100 kW. The power for optimal beam transport is ~ 65 kW; the choice of having a power of 100 kW provides a good margin to study the behaviour of the system in real applications, since power losses are difficult to predict.

To protect the cavities against pressure rises, an interlock has been installed, based on the reading of the *HV2@VS6*. If the pressure reading in the high energy cavity (FRG at *HV2@VS6*) gets worse than the set threshold (10^{-5} mbar), the RF power is lowered until the pressure gets lower than the threshold.

Just after RF-PS installation, the HF-RFQ conditioning process started and took some months to complete. Conditioning was a long but easy and straightforward process: the injected power was raised up until the pressure overcame the threshold. Power was then reduced until the pressure recovered. The process restarted and kept going until the full power could be injected and maintained for some hours at constant pressure in the permitted range (10^{-6} mbar range). Measurements showed that working at full power (100 kW peak power) is not the optimal working condition for the cavities, which is instead at 65 kW, at which there is the maximum transferred power to the cavities. This result, in perfect agreement with the optimal RF peak power calculated with the 3-D model of the HF-RFQ developed at CERN, will allow designing an improved version of the RF-PS, lighter, more compact, and less energy-consuming, which is already under study.

4 Radiation protection

As explained above, the MACHINA project aims at developing a transportable accelerator system, expected to operate at museums, conservation centres and other sites where the public can be present. Thus, MACHINA has been developed to be intrinsically safe with regard to radiation protection.

As regards the source, high voltages are limited to 20 kV. The produced X-rays, having an energy of less than 20 keV, are indeed completely absorbed in the source walls, as confirmed by extensive measurements made by the radiation protection division of the CERN laboratories, which have shown no difference from background level.

Also the accelerating cavities do not pose problems as regards radiation protection. Beam dynamics is such that only low-energy particles or un-accelerated particles can be lost. In our cavities, all lost particles are produced with an energy of less than 200 keV. The cavities are self-shielded from these particles and from the produced radiation, so no radiation is emitted. In addition, being the beam energy limited to 2 MeV, dose rates due to neutrons produced in nuclear reactions are negligible, even on copper, for which the neutron radiation has a threshold at higher energy ($E_{\text{th}}(^{65}\text{Cu}(p,n)^{65}\text{Zn}) = 2.17\text{ MeV}$). This is a point of crucial importance, as all the material which the cavities are made of is actually thick copper. All these points have been confirmed by measurements at CERN, which showed no radiation emission from the system when the beam is not extracted.

Finally, even with regard to high-energy beam transport, beam extraction and interaction with sample materials, no radio safety problems have been detected. Test measurements have been taken at the full energy and at the beam intensity typically used for CH measurements (350 pA) at LABEC, both extracting the beam in air and stopping the beam on thick samples of typical materials (plastics, aluminium, iron, and copper). The results show that there is no difference in the registered radiation dose rates when irradiating the targets with 2 MeV protons and when the beam is not accelerated (e.m. and neutron dosimeters at about $d = 35\text{ cm}$ from the target, at 0° and 50° with respect to the beam axis). For these measurements, the background level was, as usual, between 50 and 100 nSv/h for e.m. radiation and always less than 100 nSv/h for neutrons.

Following the indications of the Italian laws regarding radiation protection, MACHINA has been equipped with buttons, whose activation cuts off the HV-deck mains, thus preventing source ignition and plasma formation. In addition, the LEBT FC is normally inserted on the beam path and can be extracted only if the interlocks concerning radiation protection are active and allow the beam to proceed for acceleration.

5 Control system

The MACHINA control system has been designed and built to be user-friendly, using open-source software and highly available hardware components, with the same philosophy adopted over the course of the past ten years in our laboratory for the development of transportable instrumentation (Taccetti et al. 2019). The focus is on creating reliable systems characterised by low cost, ease of use, and easy to adapt to specific user requests, thanks to a problem-solving approach.

The control system is designed with a master/slave approach. The master (a central CPU, based on an I9 processor) communicates with distributed, independent peripherals (the turbo pump controllers and eighteen Arduino Mega 2560 boards connected in daisy chain) through RS-485 communication. The peripherals control all the devices present on MACHINA. The RS-485 link has been chosen for its robustness (immunity to noise) and ability of addressing multiple slave boards. The master PC is equipped with USB-serial RS-485 transceivers to communicate with each peripheral.

Since the Arduino boards are not equipped with serial ports for the RS-485 communication, we extended the RS-485 communication protocol to the Arduinos by installing custom shields (of the MAX family, for example the MAX1487 and MAX485) that allow data transmission/reception. These components transform the RS-485 signals into RS-232, which are then directly interpreted by the Arduinos (RX and TX pins). The command sent from the master to the single Arduino board contains a header, which is its address, followed by the task to be performed. The task can be a readout or a request to change the logic

state of a device. For example, the master can ask for the readout of the low vacuum or of the beam current intensity, while the change of a logic state can consist in the ON/OFF switch of a power supply or the OPEN/CLOSE of a valve. The addressed slave board interprets the task and sends a confirmation reply message. For example, in the case of a readout request, the reading result.

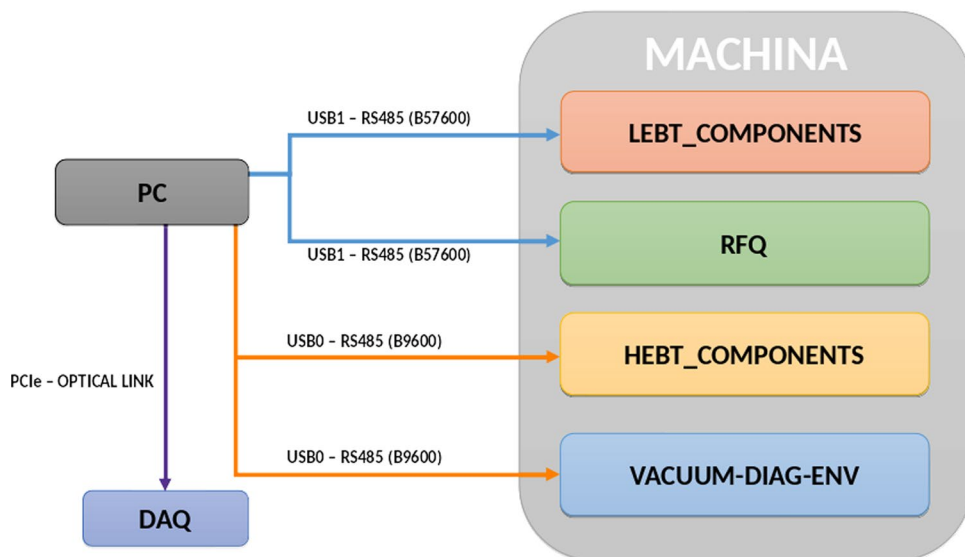
There are two lines of communication (USB0 and USB1) which differ in their data transfer rates, as described in the following.

The same master PC communicates also with the data acquisition modules (DAQ), based on CAEN digitisers, through an optical link connected by a PCIe interface. It makes available an independent data line with higher data transfer rates (bandwidths up to 100 MB/s). For the acquisition of the four detectors (three X-ray and one gamma-ray detectors), two compact CAEN DT5780 digitisers (100 MS/s, 14-bit) are installed. They provide high- and bias voltage for all the detectors and handle the signals of the detector preamplifiers. The input stage of the digitiser has been customised for a better detector signal treatment. The digitisers have very low weight (< 1 kg) and power consumption (< 45 W, which make them perfectly suited for MACHINA). The acquisition is currently under test. It is based on the hardware and software used for our XRF scanners and is going to be integrated in the MACHINA system in the next few months. The overall scheme of the MACHINA communications is shown in Fig. 6.

5.1 USB0 RS485—LINK0: vacuum, diagnostic (lebt + hebt), environment control system

USB0 is the “slow” line, devoted to the vacuum system (control and monitoring of both pumps and pressure gauges),

Fig. 6 The overall scheme of the MACHINA communication channels. LEBT_COMPO-NENTS: source and low-energy beam transport components; RFQ: radio frequency quadrupole parameters; HEBT_COM-PONENTS: high-energy beam transport components; VAC-UUM-DIAG-ENV: vacuum system, beam diagnostic and environmental parameters



beam diagnostic (FC and quartz viewer) and environmental parameters readout (power consumption, room temperature and humidity). Its data transfer speed is limited by the speed of the controllers of the turbo pumps (Agilent TWISS-TOR_84), designed to operate at a baud rate of 9600 bit/s. These controllers allow for reading the high vacuum gauges and the turbo pump parameters (temperatures, rotational speeds, absorbed powers, and status), as well as for controlling their ON/OFF settings. As regards vacuum, also the three Arduino Mega 2560 boards, one for the power on/off setting of the forepump IDP 10 and two for the readout of low-vacuum gauges, are connected to the USB0. The Arduino boards are equipped with custom shields through which they drive the devices.

The figure below shows the block diagram of the vacuum control system.

In the upper part of Fig. 7, the scheme of the control via RS485 of the high vacuum section (turbo pumps and high vacuum gauges) is shown.

In the lower part, the control of the low-vacuum section is reported. This consists of the control of the forepump status (ON–OFF, controlled by one dedicated Arduino) and the readout of four Pirani gauges (handled by two more Arduinos). The reading/change_status request is sent to the dedicated Arduino by means of the RS485 link and transformed into a RS232 command by a custom shield. As regards the Pirani pressure readings, the analogue value, corresponding

to the low-vacuum pressure, is firstly shifted for matching with the input voltage range of the ADC (MCP3201 in the picture). Then, the ADC output is sent back to the control unit and displayed to the user.

5.2 USB1 RS485—LINK1: LEBT/RFQ control system

Differently from link 0, link 1 (USB1) can work with speeds between 57.6 kb/s and 230.4 kb/s, thus allowing for a real-time control (a feature needed, for example, when optimising the source high-voltages or to have a prompt reaction of the FC to stop the beam for radio protection).

This link is in charge of controlling the peripherals of the Source, the LEBT and the RFQ PSs. As already explained in Sect. 3.1, part of the peripherals of the Source are placed on the *HV-DECK*. The communication with these elements is not as straightforward as for the elements at ground voltage, due to the almost 20 kV of potential difference between the two sides of the communication. Its main features are described in Fig. 8.

To communicate with the peripherals on the *HV-DECK*, the main PC sends a command to a custom circuit board that converts RS-485 signals to RS-232. This board transforms the TX (Transmit) electrical signals into optical, which are then fed to three optical fibres. The fibres are able to withstand tens of kV of voltage drop and can transmit the optical signals to a second board on the high-voltage deck,

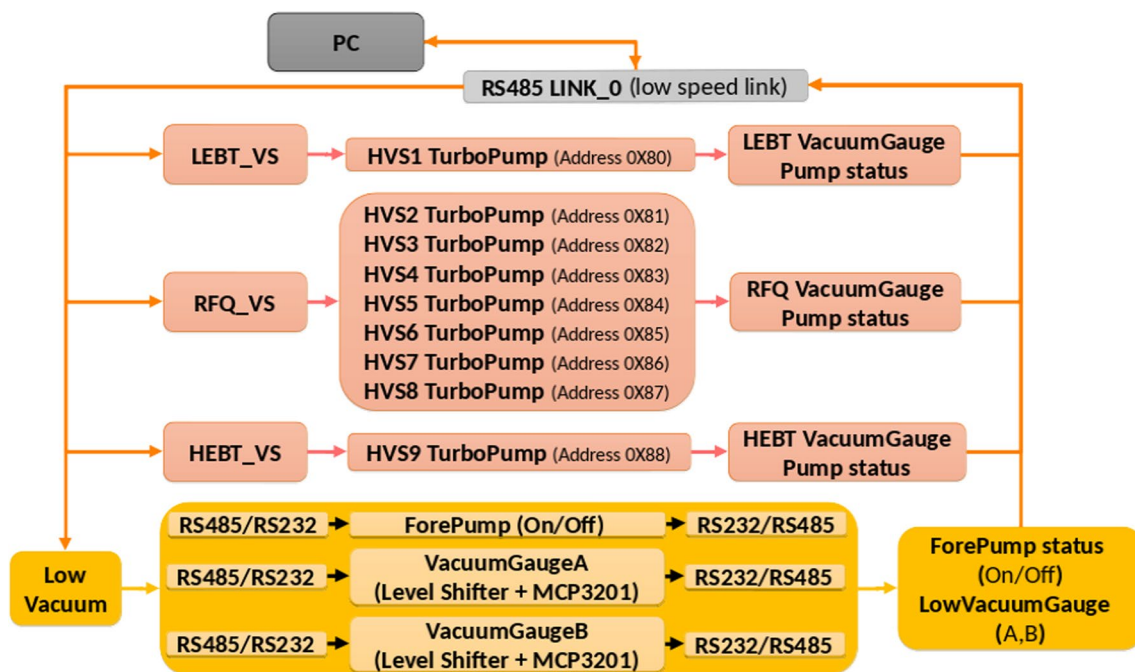
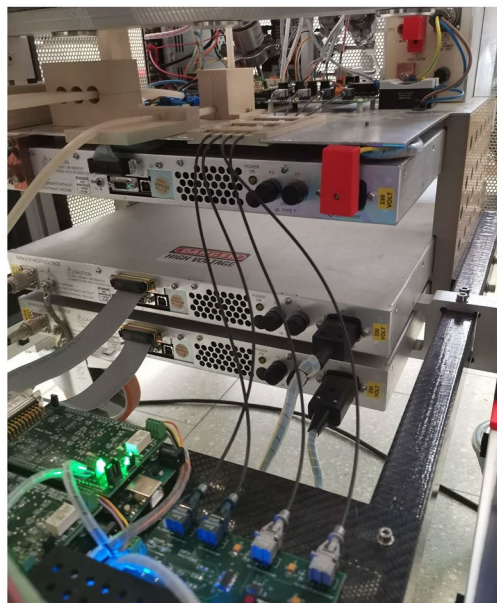
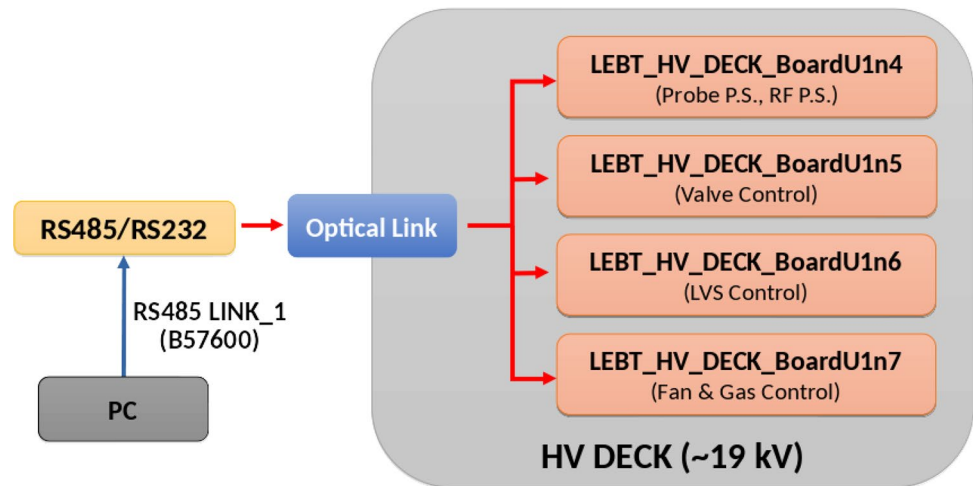


Fig. 7 Scheme of the control system of the vacuum. In the case of the low-vacuum gauge reading, shown in the lower part of the figure, the connection is not direct as in the case of the other devices (for example, the turbopumps are equipped with controllers supporting the

RS485 protocol). Here, the connection to the Arduino boards is actuated via a custom shield for each Arduino. The level shifter adapts the range of the output voltage of the low pressure gauge to the input of the ADC

Fig. 8 Top: communication scheme for the source elements at High Voltage (HV DECK) served by link1. Bottom: view of the actual implementation of the signal transmission from ground to the high-voltage deck. In the foreground, the three fibre optics for the control of the HV probe PS (the fourth is used for the emergency switch off)



which makes the reverse signal transformation from optical to electrical, buffers the transmitted data and sends it to the Arduinos on the *HV-DECK*. The Arduino in charge of executing the command replies on the RX (Receive) line with a confirmation message and with the enable signal on the ENABLE line. The HV board transforms the electrical RX and ENABLE signals into optical and sends them to the other board at ground potential. Here, the confirmation message is converted from RS-232 to RS-485 and sent to the PC, closing the loop.

5.3 MACHINA control system: software

The control software has been written using C/C++ and is based on QT 5 version 5.10 or higher (<https://doc.qt.io/>

qt-5/). The software runs in a Linux environment. It is based on eight stand-alone programs, interlaced with each other through the use of shared memory, as shown in Fig. 9.

All the modules (vacuum, LEBT, HEBT, Miscellanea, RFQ) can be accessed separately through the general window. In Fig. 10, a screenshot of the vacuum panel is reported.

Indeed, the vacuum panel is the first one to be accessed and all the connected devices have to be fully responding before opening any further module. Actually, as the “good vacuum” is a mandatory condition to operate the accelerator, as a first step all the VSs have to be able to communicate, be switched on and have reached the full operating condition (i.e. must be in the “normal” status), and all the vacuum gauges active and transmitting.

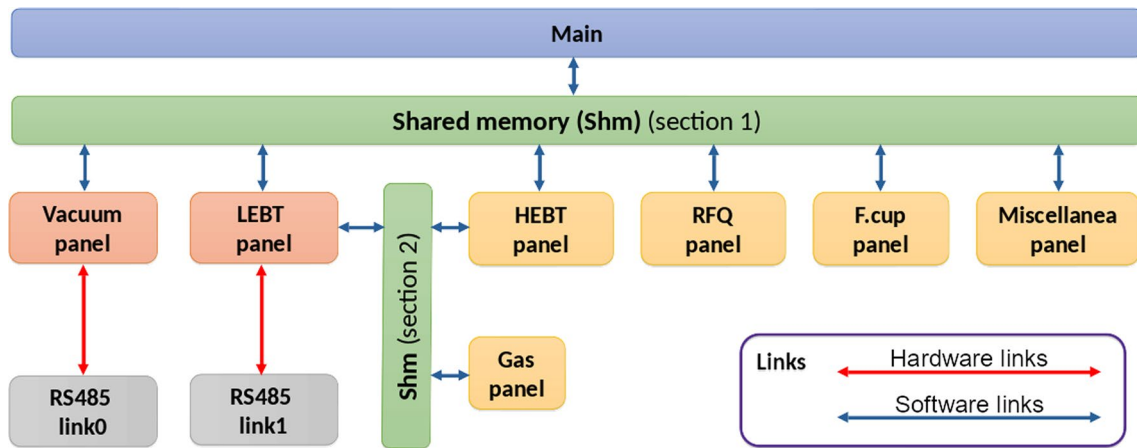
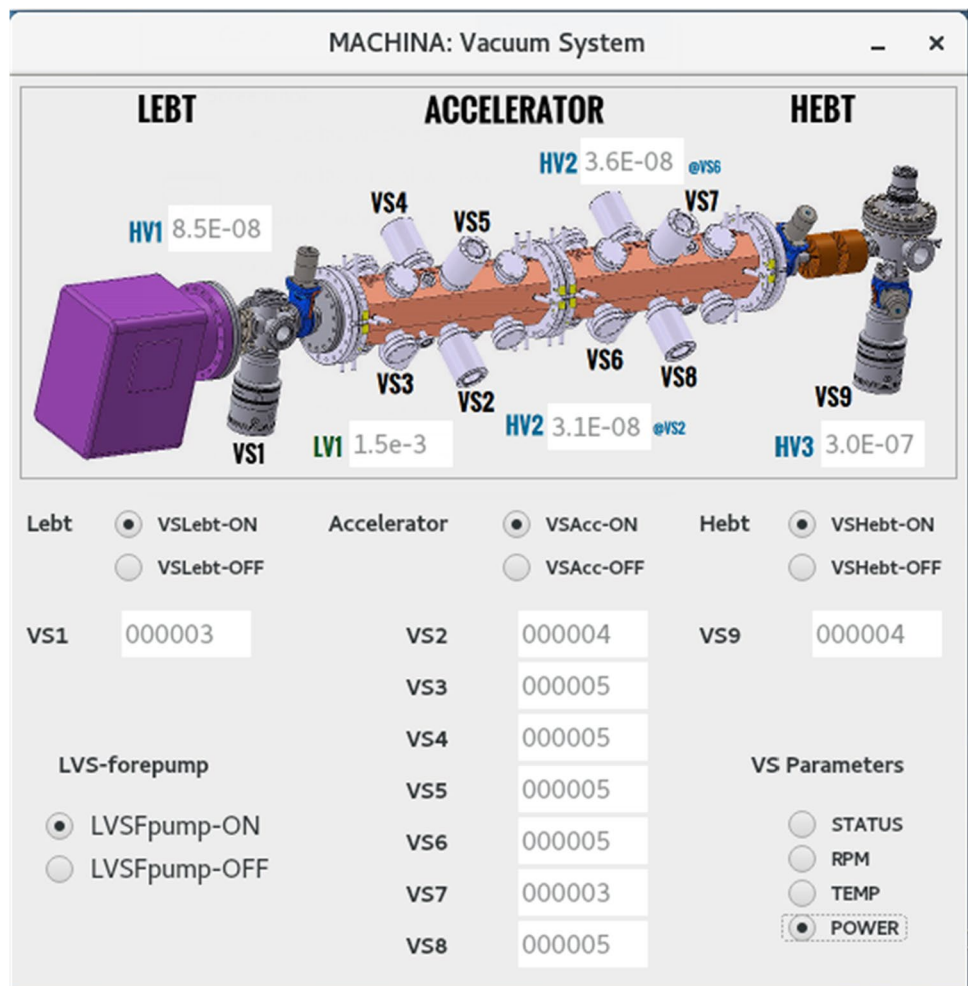


Fig. 9 The functional structures of the software and the hardware links are represented in the picture. The program interconnections are based on the shared memory

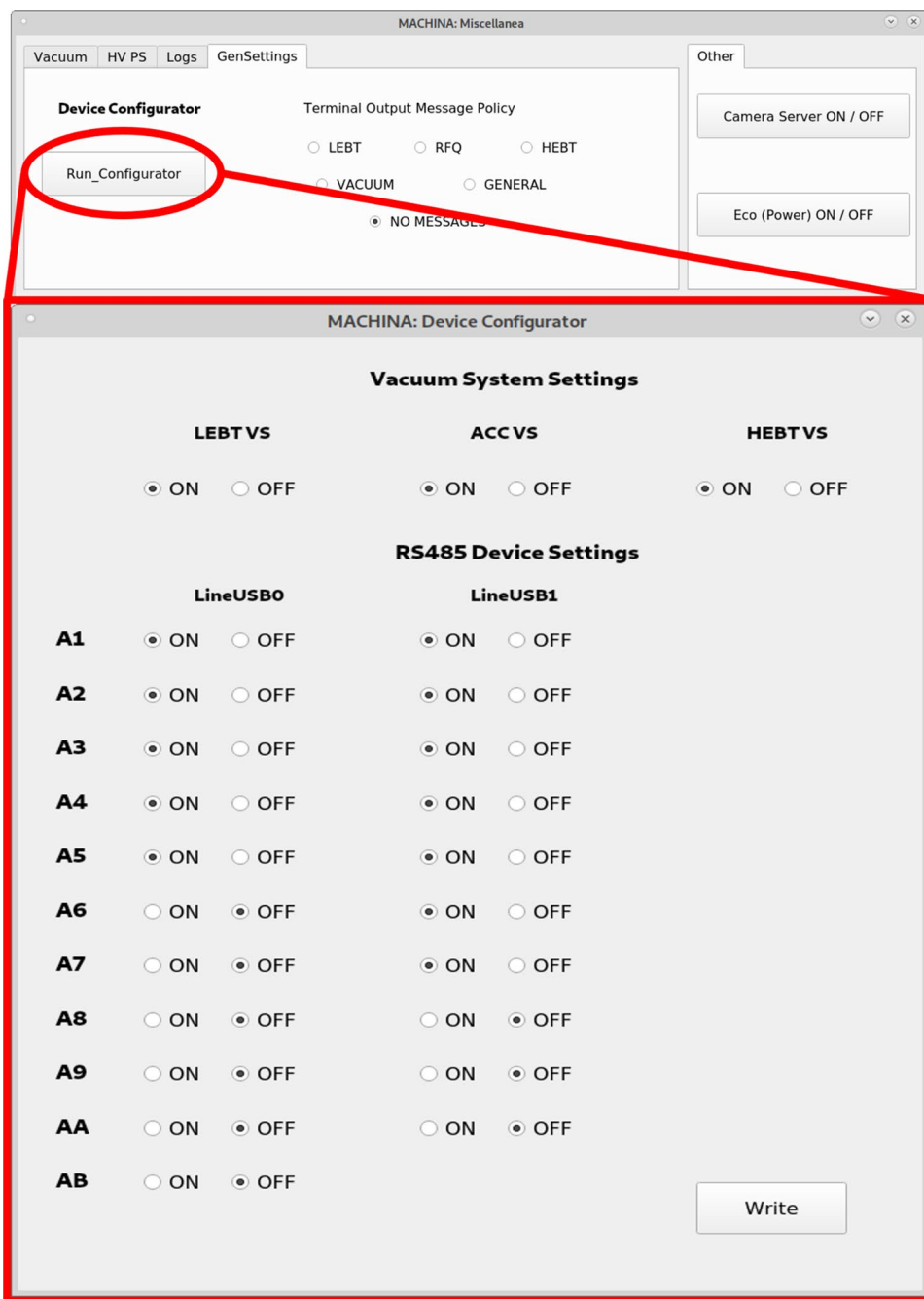
Fig. 10 The vacuum panel is open and shows the vacuum reading (*LV1, HV1, HV2, HV3*, the low- and high-vacuum readouts) and VS parameters (in this image, the ON/OFF status of all the pumps and the absorbed power (W) of all the turbopumps are shown)



The vacuum panel is the part of the control software with direct access to link0, while LEBT panel has direct access to link1. All other programs communicate with

vacuum and LEBT through the control PC shared memory in order to have access to the USB links. *LV1* in the panel

Fig. 11 The Miscellanea panel where it is possible to enable or disable the communication to any controller (Arduino, turbopump controller). To be more compact, the controllers are indicated with a letter and a number for each communication line. When passing over with the mouse indicator, the programs prompt the full name of the corresponding section (e.g. *VSI*, *HV2*, etc.), thus allowing for an easy identification of the desired item



indicates a Pirani gauge readout along the turbopump exhaust line (the one close to the *VSI*).

On the Miscellanea panel, shown in Fig. 11, it is possible to enable or disable the communication to any controller (Arduino, turbopump controller). This feature was introduced in order to identify the peripheral(s) which are, for example, malfunctioning or need maintenance, or in case it is necessary to improve/change/update parts of the system

and it is not possible to switch off the whole system. This feature has proved its usefulness many times.

The gas panel allows controlling all the gas transport system, from the high-pressure vessel to the injection into the source bottle. The LEBT panel is dedicated to the control of all the source parameters and to the control/readout of the Faraday Cup just downstream of the source. In the following, the gas system and the LEBT panels, which are

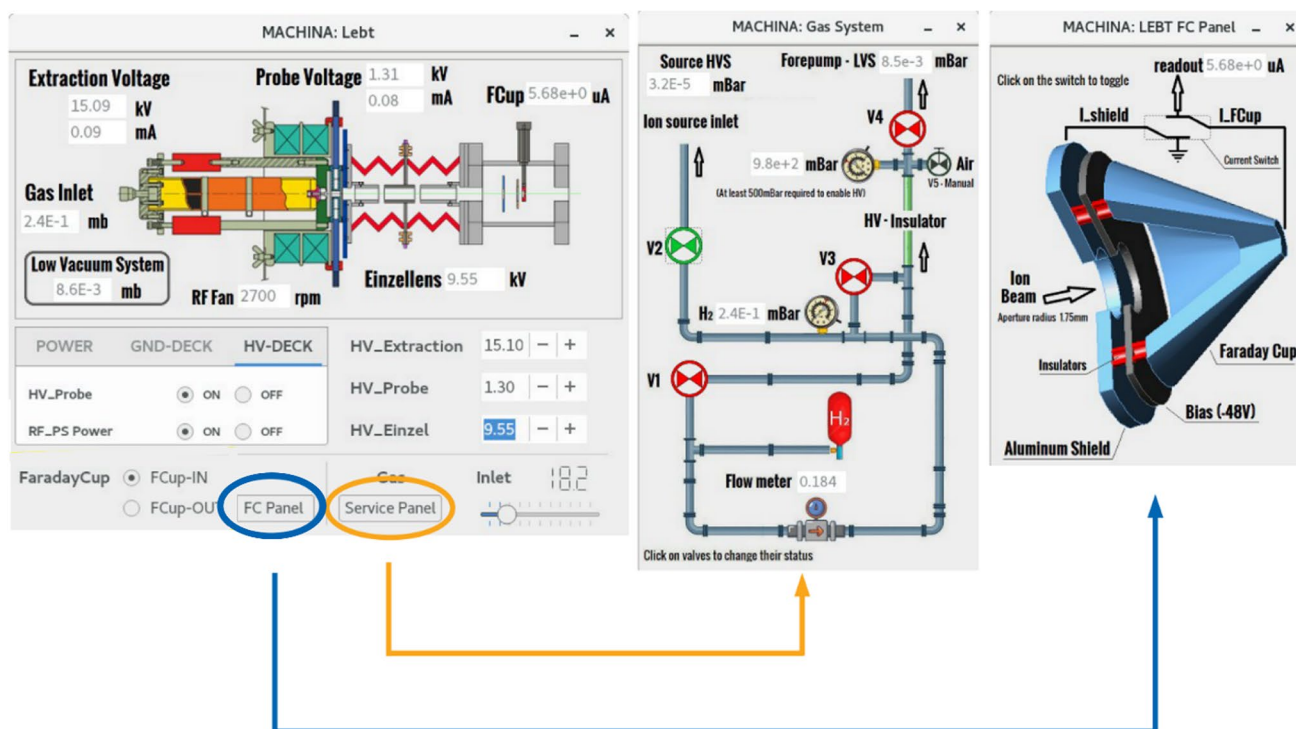


Fig. 12 Left: the source/LEBT control panels. It provides full control over the source settings (HV_Extraction, HV_Probe, HV_Einzel, RF PS On/OFF status, hydrogen mass flow) and readouts (Extraction current, Probe current, Fan speed, hydrogen pressure in the line from the mass flow controller to the quartz bottle, the foreline pressure at the entrance of the scroll pump, the current in the Faraday Cup downstream of the source). Centre: the Gas System control panel. It allows

controlling all the valve (V1, V2, V3 and V4) status along the gas path (red = close, green = open). In the picture, as the source is running, the V2 valve is open and the others closed. Right: the LEBT Faraday Cup control panel, where either the current stopped in the front shield or the current injected into the Faraday cup can be measured (In the picture, the shield current is discharged to ground, the FC current, 5.68 μA , is read)

necessarily interlinked and need to work together, are shown and described.

The gas system panel (middle, Fig. 12), accessed by the Service *panel* push button in the LEBT panel, allows:

- Opening/closing the valves V1, V2, V3 and V4 (red = close, green = open), which allow either the gas to flow into the source (V1 and V2) or to connect the gas line to an external HV system (V3 and V4);
- Reading the hydrogen mass flow (*Flow meter*, 0.184);
- Reading the gas pressure in the gas pipe towards the source bottle, after the flow controller (H_2 2.4E-1 mbar);
- Reading the hydrogen pressure in the high-pressure bottle (9.8E+2 mbar)
- Reading the actual pressure downstream of the source (*Source HVS* 3.2E-5 mbar).

The LEBT panel (left, Fig. 12) allows:

- Controlling the mass flow meter. In the LEBT panel, low-right corner, the sliding bar to change the flow is shown together with the set value (*Gas Inlet* 18.2% of the maximum flow);

- Switching on the fan cooling the source and monitoring its speed (*RF Fan* 2700-rpm);
- Powering the *GND-DECK* and the *HV-DECK*;
- Switching on the HV_Extraction and the HV_Einzel PSs (both on the *GND-DECK*), the HV-Probe (*HV-DECK*, shown in the active tab of Fig. 12), set the three high voltages (15.10, 9.55, and 1.30 kV respectively), and switch on the RF PS (shown in the active tab of Fig. 12);
- Controlling the IN/OUT position of the LEBT Faraday Cup *FC* (IN in Fig. 12) and opening the dedicated FC panel, shown in Fig. 12, left (LEBT FC panel).

The LEBT *FC* panel allows reading either the frontal shield current or the actual FC-current (*readout* 5.68e+0 μA in Fig. 12, right), measured behind the biased frontal shield.

The RFQ panel allows for powering the RF power supply and monitoring the temperatures of the water along the RFQ cooling lines.

From the HEBT panel, we can remotely control the stepper motor of the rotatable carousel of the diagnostic station (described in par 3.3 HEBT). In this panel, the readout of

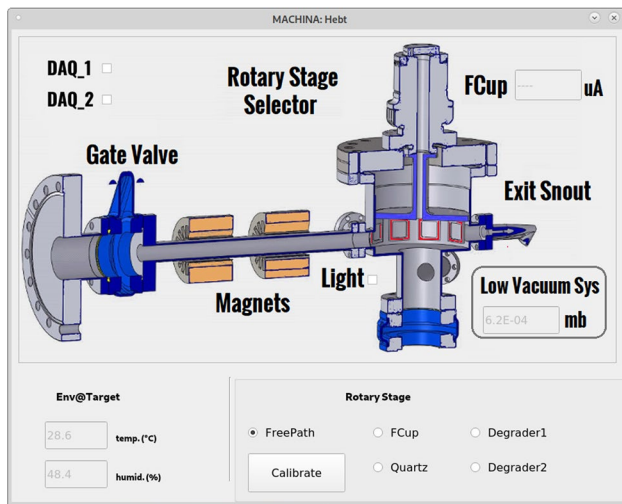


Fig. 13 Scheme of the HEBT section control panel. It allows measuring the environmental temperature/humidity, the current in the high-energy Faraday Cup and controlling the *Rotary Stage Selector*. This element controls the position of the rotatable carousel inside the high-energy diagnostic chamber. Changing the position of the carousel allows inserting along the beam path any of the two energy degraders, the beam quartz viewer, the high-energy Faraday Cup. When the FreePath position is chosen, the beam is free to proceed towards the extraction windows and eventually to reach the target

the FC current and the environmental parameters (humidity (48.4%) and temperature (28.6 °C) in the accelerator room) are displayed, as shown in Fig. 13. It also allows for switching on/off the LED lights to light up the diagnostic chamber.

6 Beam tests

The source alone, first, and then the source and the accelerator assembly, have been tested. Hereafter, we shortly report on the performed tests and their results.

6.1 Source beam tests

For characterising the beam at the entrance of the accelerator (i.e. about 30 cm downstream of the source exit canal), an acceptance box (AB) has been designed and built at CERN for the PIXE-RFQ, and it has the same acceptance of the accelerator. This system was developed for the Linac4 source (Lallement et al. 2018). It consists of a Faraday Cup preceded by 4 transverse collimators (masks). The aperture size and the relative position of the masks are calculated such that only the particles inside the RFQ acceptance can pass into the Faraday cup and thus contribute to the measured current. The entrance of the RFQ corresponds to a position located a few millimetres from the second mask. This system allows a fast and easy optimisation of the source and LEBT parameters.

The structure of the AB is reported in Fig. 14, where the Faraday Cup and the four concentric diaphragms with square apertures (4 mm, 1 mm, 1 mm, 4 mm side respectively), allowing to define the AB acceptance, are shown.

For the test measurements, the AB was mounted on a linear shift positioner to allow movement (50 mm travel range, 0.1 mm sensitivity) along the beam axis, as shown in Fig. 15.

To prevent the loss of low-energy secondary electrons, which can produce systematic errors in the measurement of the current collected by the Faraday cup, a positive bias has been used. When the bias voltage is changed from 0 V to +100 V, there is a factor two fall in the current reading, due to secondary electron suppression, while from +100 V up (the maximum available in our set-up being +200 V), the current reading stays constant.

Simulations have shown that at the first mask, the beam area is about ten times bigger (170 mm² area) than the area of the mask aperture (16 mm² area), which corresponds to a beam diameter roughly 3 times bigger than the mask aperture (13-mm expected beam size with respect to a hole size of 4 mm). So, when the beam is centred on the first diaphragm and the axes of the source and the AB are aligned, it is expected that the beam can be displaced along the X and Y axes for a few millimetres without noticeable variations of the transmitted beam intensity.

Tests were carried out to study the source-to-accelerator positioning, and it was not possible to find the flat top region of beam intensity versus source displacement (horizontal, vertical, and tilting angles in the two planes). This was due to an insufficient range of the possible displacements, both linear and angular. So, a new supporting structure was built, which allows for wider linear (about ±20 mm left/right and bottom/up) and tilting adjustments (about ±15° degrees). The new configuration allowed optimising the source-to-accelerator coupling and thus to obtain a configuration rather insensitive to small variation of the source-to-accelerator mutual positioning.

6.2 Accelerated beam tests

In March 2022, all the MACHINA subsystems had been successfully completed and it was possible to test the whole system. The used configuration was as follows.

Source parameters: 16.72 kV extraction, 3.28 kV probe and 14 kV Einzel lens voltages, with the gas flowmeter set at about 8% of the full scale. Pressure: in the low part of 10⁻⁵ mbar in the LEBT, mid 10⁻⁶ mbar scale in the cavities and well within the 10⁻⁷ mbar scale in the HEBT.

Duty-cycle parameters (waveform generator): trapezoidal signal between -1 V (base) and 3 V (flat-top), 125 μs FWHM length, 5 ms repetition rate; 749.285 MHz signal generator frequency.

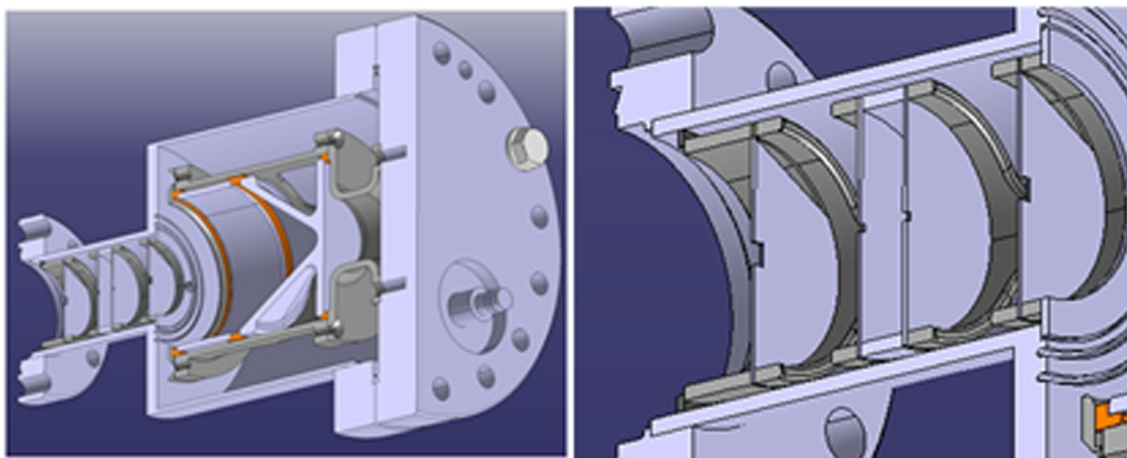


Fig. 14 Left-hand side: cross-section of the AB. Right-hand side: blow up of the diaphragms and the apertures defining the beam divergence

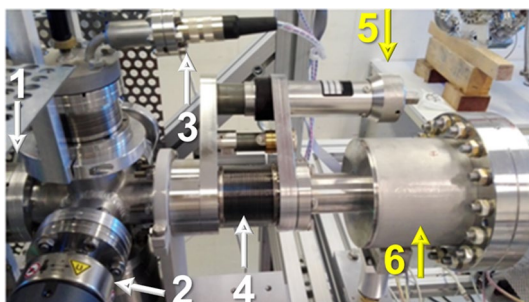


Fig. 15 Lateral view of the Acceptance Box. The beam comes from the left. From left: the 6 ways cross (1-the flange where the 6 ways cross is connected to the source; 2-the HV1 gauge; 3-the connector for the readout of the measured currents and for biasing the LEPT FC), 4-the bellow and 5-the knob of the linear shift positioner, which allows sliding back and forth the AB with respect to the source; 6-the AB

In these conditions, we had a bright beam, with a mean current intensity higher than 150 pA, rather a standard value for measurements in the CH field (Grassi et al. 2007). It should be noticed that such a current density (about 250 pA/mm², integrated over 300 s, a typical measurement time) can be used only with “robust” samples, in order to have safe measurements for the object under study. However, significantly lower beam currents may be used still keeping sufficiently high statistics. The used set-up is shown in Fig. 16, together with the images of the luminescence induced on a synthetic sapphire by the extracted beam.

These tests, although absolutely preliminary, show that the MACHINA project has successfully met its objectives. The detection system, both as regards detector assembly and acquisition software, is now ready to be added to MACHINA. Within the end of 2022, the whole system (accelerator and detection system) is expected to be

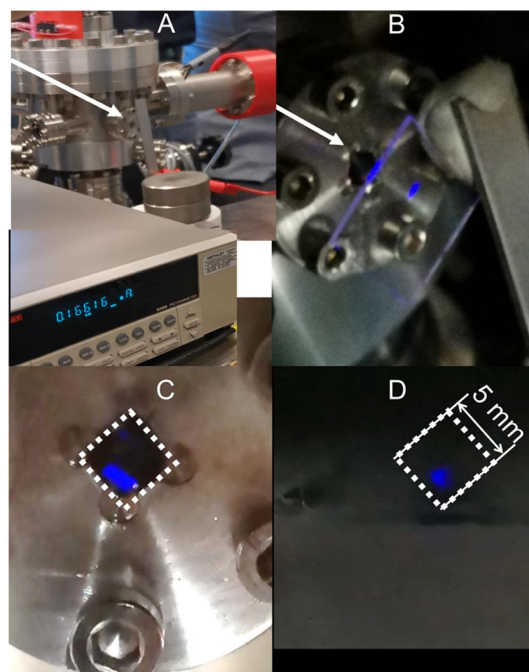


Fig. 16 Top row. **A**: the final part of the beamline (the white arrow suggests the beam path). From left: the diagnostic chamber with the flange holding the Si₃N₄ window (hardly visible just in front of the point of the arrow), a vertical metal stripe (grey) mounted on an insulating support (white disk), connected by the red crocodile clip to the picoammeter (visible in the foreground while measuring about 150 pA current). **B**: blow up (side view) of the extracted beam fluorescence induced in a synthetic sapphire (20×20×2 mm³), whose borders can be viewed due to the light transported along the sapphire. Bottom row: magnified views, along the beam axis, of the fluorescence induced by the beam in the sapphire (not distinguishable here), after passing through the extraction window (outlined by the white dashed squares). **C**: front view of the beam spot on the sapphire before optimising the positions of the two PMQs. **D**: same view, after PMQs optimisation. The size of the window allows estimating the spot size to ~0.8 mm diameter

operative and able to carry out first tests on CH objects, first at the INFN-LABEC and then at the OPD conservation laboratory.

7 Conclusions

The joint INFN-CERN MACHINA project, born after a friendly discussion in mid-2017, was presented by INFN to the Italian Ministry of University and Research and financed, after a competitive evaluation, by the end of the same year (FISR-Fondo Integrativo Speciale per la Ricerca 2017). CERN-KT sponsored the development of the PIXE-RFQ. 2018 was largely dedicated to the acquisition of the material and instrumentations and to set up a dummy accelerator, used to test the vacuum system, and a vacuum chamber to test the source. Unfortunately, 2020 and 2021 were dominated by the problems connected with the pandemic, and the experimental work was noticeably hampered. During this period, we improved the control electronics and software and designed the second-generation supporting structure. The integration of the HF-RFQ PS in the system was delayed until October 2021, when the whole system was completed and we were able to start conditioning the cavities. At the rise of 2022, we could finally start testing the system and, in March 2022, we finally got the first extracted 2 MeV proton beam.

The main points of the work done so far are:

- MACHINA met all its objectives in developing a simple, robust, reliable, user-friendly, autonomous, and transportable system for IBA analysis;
- All the hardware and software subsystems were developed, tested, assembled and are now in their final configuration;
- The RF power supplies have been installed and allowed finding the optimal configuration for routine use. A next-generation RF power supply system, lighter and more compact, is already under study;
- The whole system proved its transportability, being moved back and forth between the INFN-LABEC in Florence and CERN in Geneva many times;
- Both the detector assembly and acquisition software are ready to be added to MACHINA;
- Measurements have shown that MACHINA is intrinsically safe, as radiation protection is concerned. This is a point of crucial importance to make it possible to use MACHINA at museums, conservation centres and sites where the public can be present.

The complete version of MACHINA is going to be operational within 2022. By the fall of 2022, the first IBA

measurements on reference standard samples, of certified areal thickness and composition, and on test artworks from the OPD will be carried on at the INFN-LABEC laboratory.

The accelerator will then be transferred to the OPD, to become part of the instrumentation normally used in the diagnostic activity, in 2023.

Acknowledgements The authors acknowledge INFN-CHNet, the network of laboratories of the INFN for CH, for support and precious contributions in terms of instrumentation and personnel. F. Taccetti and L. Giuntini wish to thank L. Sodi for assistance and suggestions for the mechanics of the project. L. Zuccalà is also thanked with gratitude for the many useful discussions, which helped to produce a better and clearer description of the project.

Author contribution All authors contributed to the study conception and design. Material preparation, data collection and analysis were carried out thanks to the contribution of all the authors. The first draft of the manuscript was written by FT and LG and all authors commented on previous versions of the manuscript. All authors read and approved the final manuscript.

Funding This work was supported by the Italian FISR (Fondi Speciali per la Ricerca from the Ministry of Education, University and Research, prot. n. 0021264 of 21 December 2017) and by the CERN Knowledge Transfer Fund.

Data availability The datasets generated during and/or analysed during the current study are available from the corresponding author on reasonable request.

Declarations

Conflict of interest The authors have no competing interests to declare that are relevant to the content of this article.

Open Access This article is licensed under a Creative Commons Attribution 4.0 International License, which permits use, sharing, adaptation, distribution and reproduction in any medium or format, as long as you give appropriate credit to the original author(s) and the source, provide a link to the Creative Commons licence, and indicate if changes were made. The images or other third party material in this article are included in the article's Creative Commons licence, unless indicated otherwise in a credit line to the material. If material is not included in the article's Creative Commons licence and your intended use is not permitted by statutory regulation or exceeds the permitted use, you will need to obtain permission directly from the copyright holder. To view a copy of this licence, visit <http://creativecommons.org/licenses/by/4.0/>.

References

- Alfeld M, de Viguier L (2017) Recent developments in spectroscopic imaging techniques for historical paintings—a review. *Spectrochim Acta Part B* 136:81–105. <https://doi.org/10.1016/j.sab.2017.08.003>
- Awad WM, Biais M (2020) How mobile NMR can help with the conservation of paintings. *Magn Reson Chem* 58(9):792–797. <https://doi.org/10.1002/mrc.5071>
- Calligaro, T., Arean, L., Pacheco, C., Lemasson, Q., Pichon, L., Moignard, B., Boust, C., (2020), Heirich, V., A new 3D positioner for the analytical mapping of non-flat objects under accelerator beams,

- Nucl. Instrum. Methods Phys. Res. B, 467, 65–72, <https://doi.org/10.1016/j.nimb.2020.01.028>
- Chiari, M., Barone, S., Bombini, A., Calzolari, G., Carraresi, L., Castelli, L., Czelusniak, C., (2021), Mandò, P.A., LABEC, the INFN ion beam laboratory of nuclear techniques for environment and cultural heritage. European Physical Journal Plus 136 (4) 472, <https://doi.org/10.1140/epjp/s13360-021-01411-1>
- D'Alvia L, Pittella E, Rizzuto E, Piuze E, Del Prete Z (2022) A portable low-cost reflectometric setup for moisture measurement in cultural heritage masonry unit, measurement, 189. ISSN 110438:0263–2241. <https://doi.org/10.1016/j.measurement.2021.110438>
- Defeyt C, Walter P, Rousselière H, Vandenabeele P, Vekemans B, Samain L, Strivay D (2017) New Insights on Picasso's blue period painting La famille soler. Stud Conserv 63(1):24–35. <https://doi.org/10.1080/00393630.2017.1361628>
- Dimov V.A., Caldara M., Degiovanni A., Esposito L.S., Fink D.A., Giunta M., Jeff A., Valloni A., Lombardi A.M., Mathot S.J., Vretenar M., (2018) Beam commissioning of the 750 MHz proton RFQ for the LIGHT prototype, 9th International Particle Accelerator Conference (IPAC2018), Vancouver, BC, Canada, JACoW, Geneva, Switzerland 658–660, <https://doi.org/10.18429/JACoW-IPAC2018-TUPAF002>
- Dran J.C., Salomon J., T. Calligaro, P. (2004) Walter, Nucl. Instrum. Methods Phys. Res. B, 219–220, 7–15, <https://doi.org/10.1016/j.crhy.2009.09.001>
- Duval, A., Guicharnaud, H., Dran, J.C., Particle induced X-ray emission: A valuable tool for the analysis of metalpoint drawings, (2004) Nucl. Instrum. Methods Phys. Res. B, 226 (1-2), pp. 60–74, <https://doi.org/10.1016/j.nimb.2004.02.020>
- Gilbert, B., Denoël, S., Weber, G., Allart, D., (2003) Analysis of green copper pigments in illuminated manuscripts by micro-Raman spectroscopy, Analyst, 128 (10) 1213–1217, <http://pubs.rsc.org/en/journals/journal/an>, <https://doi.org/10.1039/b306138h>
- Giuntini L, Massi M, Calusi S (2007) The external scanning proton microprobe of Firenze: a comprehensive description, Nucl. Instrum. Methods Phys. Res. A 576, 2–3, 266–273, ISSN 0168–9002, <https://doi.org/10.1016/j.nima.2007.03.021>
- Grassi N (2009) Differential and scanning-mode external PIXE for the analysis of the painting Ritratto Trivulzio by Antonello da Messina. Nucl. Instrum. Methods Phys. Res. B, 267:825. <https://doi.org/10.1016/j.nimb.2008.12.018>
- Grassi N, Migliori A, Mandò PA, Calvo del Castillo H (2005) Differential PIXE measurements for the stratigraphic analysis of the painting madonna dei fusi by Leonardo da Vinci. X-Ray Spectrom 34:306. <https://doi.org/10.1002/xrs.821>
- Grassi N, Giuntini L, Mandò PA, Massi M (2007) Advantages of scanning-mode ion beam analysis for the study of cultural heritage. Nucl. Instrum. Methods Phys. Res. B, 256:712–718. <https://doi.org/10.1016/j.nimb.2006.12.196>
- Grazzi, F., Cialdai, C., Manetti, M., Massi, M., Morigi, M.P., Bettuzzi, M., Brancaccio, R., (2021), Giuntini, L., A multi-technique tomography-based approach for non-invasive characterization of additive manufacturing components in view of vacuum/UHV applications: preliminary results Rend Fis Acc Lincei, 32 (3) 463–477, <https://doi.org/10.1007/s12210-021-00994-2>
- Jehlička, J., Culka, A., (2022) Critical evaluation of portable Raman spectrometers: From rock outcrops and planetary analogs to cultural heritage – A review, Analytica Chimica Acta, 1209, art. 339027, <http://www.journals.elsevier.com/analytica-chimica-acta>, <https://doi.org/10.1016/j.aca.2021.339027>
- Lallement J.-B., Bencini V., Bertolo S., Di Lorenzo F., Lettry J., Lombardi A., Mastrostefano C., Noll D., O'Neil M., (2018) Activities at the Linac4 Test Stand, 29th International Linear Accelerator Conference, <https://doi.org/10.18429/JACoW-LINAC2018-TUPO127>, TUPO127
- Liss, B., Stout, S. (2017). Materials Characterization for Cultural Heritage: XRF Case Studies in Archaeology and Art. In: Vincent, M., López-Menchero Bendicho, V., Ioannides, M., Levy, T. (eds) Heritage and archaeology in the digital age. quantitative methods in the humanities and social Sciences. Springer, Cham. https://doi.org/10.1007/978-3-319-65370-9_3
- Lombardi, A.M., Dimov, V.A., Garlasche, M., Grudiev, A., Mathot, S., Montesinos, E., Myers, S., (2015), Vretenar, M., Beam dynamics in a high frequency RFQ, 6th International Particle Accelerator Conference, IPAC 2015, 2408–2412, <http://accelconf.web.cern.ch/AccelConf/IPAC2015/html/sessi0n.htm>, ISBN: 978–395450168–7
- Lucarelli, F., Calzolari, G., Chiari, M., Nava, S., Carraresi, L., Study of atmospheric aerosols by IBA techniques: The LABEC experience 2018 Lucarelli, F., Calzolari, G., Chiari, M., Nava, S., Carraresi, L., Study of atmospheric aerosols by IBA techniques: The LABEC experience, (2018) Nucl. Instrum. Methods Phys. Res. B, 417 121-127, <https://doi.org/10.1016/j.nimb.2017.07.034>
- Marucci, G., Beeby, A., Parker, A.W., Nicholson, C.E., (2018) Raman spectroscopic library of medieval pigments collected with five different wavelengths for investigation of illuminated manuscripts, Analytical Methods, 10 (10) 1219–1236. <http://pubs.rsc.org/en/journals/journal/ay>, <https://doi.org/10.1039/c8ay00016f>
- Mathot, S., Anelli, G., Atieh, S., Bilton, A., Bulat, B., Callamand, T., Calvo, S., (2019), Giuntini, L. The CERN PIXE-RFQ, a transportable proton accelerator for the machina project, Nucl. Instrum. Methods Phys. Res. B, 459, pp. 153-157, <https://doi.org/10.1016/j.nimb.2019.08.025>
- Mazzinghi, A., Ruberto, C., Castelli, L., Ricciardi, P., Czelusniak, C., Giuntini, L., Mandò, P.A., (2021), Taccetti, F., The importance of being little: MA-XRF on manuscripts on a Venetian island, X-Ray Spectrometry, 50 (4) 272–278, <http://onlinelibrary.wiley.com/journal>, [https://doi.org/10.1002/\(ISSN\)1097-4539](https://doi.org/10.1002/(ISSN)1097-4539), <https://doi.org/10.1002/xrs.3181>
- A.-M. B Olsson, T Calligaro, S Colinart, J.C Dran, N.E. G Lövestam, B Moignard, J Salomon, Micro-PIXE analysis of an ancient Egyptian papyrus: Identification of pigments used for the "Book of the Dead" 2001 Micro-PIXE analysis of an ancient Egyptian papyrus: Identification of pigments used for the "Book of the Dead", (2001) Nucl. Instrum. Methods Phys. Res. B, 181 (1–4), pp. 707–714, [https://doi.org/10.1016/S0168-583X\(01\)00545-6](https://doi.org/10.1016/S0168-583X(01)00545-6)
- Milota, P., Reiche, I., Duval, A., Forstner, O., Guicharnaud, H., Kutschera, W., Merchel, S., (2008), Golser, R., PIXE measurements of Renaissance silverpoint drawings at VERA, Nucl. Instrum. Methods Phys. Res. B, 266 (10) 2279-2285, <https://doi.org/10.1016/j.nimb.2008.03.005>
- Oliveira R, de Paula A, Gonçalves F, Bueno R, Calgam T, Azeredo S, Araújo O, A. Machado A, Anjos M, Lopes R, Oliveira D (2022) Development and characterization of a portable CT system for wooden sculptures analysis, Radiation Physics and Chemistry, Development and characterization of a portable CT system for wooden sculptures analysis. 110409, ISSN 0969–806X, <https://doi.org/10.1016/j.radphyschem.2022.110409>
- Olsson, A.-M., Calligaro, T., Colinart, S., Dran, J.C, Lövestam, N.E.G, Moignard, B., Salomon, J. Lebon, M., Pichon, L., Beck, L., Enhanced identification of trace element fingerprint of prehistoric pigments by PIXE mapping, (2018) Nucl. Instrum. Methods Phys. Res. B, 417 91–95, <https://doi.org/10.1016/j.nimb.2017.10.010>
- Pouyet, E.; Barbi, N.; Chopp, H.; Healy, O.; Katsaggelos, A.; Moak, S.; Mott, R.; Vermeulen, M.; Walton, M. Development of a highly mobile and versatile large MA-XRF scanner for in situ analyses of painted work of arts. X-ray Spectrom. 2020, 1–9, <https://dx.doi.org/10.1002/xrs.3173>

- Ravaud E, Pichon L, Laval E, Gonzalez V, Eveno M, Calligaro T (2018) Development of a versatile XRF scanner for the elemental imaging of paintworks. *Microchem J* 137:277–284. <https://doi.org/10.1007/s00339-015-9522-4>
- Riminesi C, Cuzman OA, Moczko M, Raszczuk K (2022) Comparative interpretation of results after application of different non-destructive and portable techniques on historic concrete in the centennial hall in wrocław, case studies in construction materials, ISSN e01409 2214-5095, <https://doi.org/10.1016/j.cscm.2022.e01409>
- Roascio S, Zucchiatti A, Prati P, Cagnana A (2002) Study of the pigments in medieval polychrome architectural elements of “Veneto-Byzantine” style. *J Cult Herit* 3(4):289–297. [https://doi.org/10.1016/S1296-2074\(02\)01239-6](https://doi.org/10.1016/S1296-2074(02)01239-6)
- Romano, F.P., Pappalardo, L., Calvi, G., Costa, E., Marchetta, C., Pappalardo, G., Rizzo, F., Russo, S., (2012), A new version of a portable polonium source for the non-destructive PIXE (particle induced X-ray emission) analysis in the cultural heritage field *Microchemical Journal*, 101 95–98, <https://doi.org/10.1016/j.microc.2011.11.007>
- Rousaki, A., Vandenabeele, P., (2021) In situ Raman spectroscopy for cultural heritage studies, *Journal of Raman Spectroscopy*, 52 (12) 2178–2189, [http://onlinelibrary.wiley.com/journal/https://doi.org/10.1002/\(ISSN\)1097-4555](http://onlinelibrary.wiley.com/journal/https://doi.org/10.1002/(ISSN)1097-4555), <https://doi.org/10.1002/jrs.6166>
- Senesi GS, Harmon RS, Hark RR (2021) Field-portable and handheld laser-induced breakdown spectroscopy: Historical review, current status and future prospects. *Spectrochimica Acta part B - atomic spectroscopy*. <https://doi.org/10.1016/j.sab.2020.106013>
- Taccetti F, Castelli L, Czelusniak C, Gelli N, Mazzinghi A, Palla L, Ruberto C, Censori C, Lo Giudice A, Re A et al (2019) A multi-purpose X-ray fluorescence scanner developed for in situ analysis. *Rend Fis Acc Lincei* 30:307–322. <https://doi.org/10.1007/s12210-018-0756-x>
- Vandenabeele P, Donais MK (2016) Mobile spectroscopic instrumentation in archaeometry research. *Appl Spectrosc* 70(1):27–41. <https://doi.org/10.1177/0003702815611063>
- Qt is a full development framework with tools designed to streamline the creation of applications and user interfaces for desktop, embedded, and mobile platforms. <https://doc.qt.io/qt-5/>
- Ziegler JF, Ziegler MD, Biersack JP (2010) SRIM – The stopping and range of ions in matter, *Nucl. Instrum. Methods Phys. Res. B*, 268 1818–1823, <https://doi.org/10.1016/j.nimb.2010.02.091>
- Zucchiatti, A., Climent-Font, A., García Gómez-Tejedor, J., Martina, S., Muro García, C., Gimeno, E., Hernández, P., (2015), Canelo, N., Building a fingerprint database for modern art materials: PIXE analysis of commercial painting and drawing media) *Nucl. Instrum. Methods Phys. Res. B*, 363, 150–155, <https://doi.org/10.1016/j.nimb.2015.08.076>

Publisher's Note Springer Nature remains neutral with regard to jurisdictional claims in published maps and institutional affiliations.